Submitted to

International Europhysics Conference on High Energy Physics, EPS03, July 17-23, 2003, Aachen
(Abstract **105** Parallel Session **13**)

XXI International Symposium on Lepton and Photon Interactions, LP03, August 11-16, 2003, Fermilab

www-h1.desy.de/h1/www/publications/conf/conf_list.html

A Search for Leptoquark Bosons in ep Collisions at HERA

H1 Collaboration

Abstract

A search for scalar and vector leptoquarks coupling to first generation fermions is performed in the H1 experiment using e^+p and e^-p data collected from 1994 to 2000. No significant evidence for the direct production of such particles is found in a data sample with a large transverse momentum final state electron or with large missing transverse momentum, and constraints on leptoquark models are established. For leptoquark couplings of electromagnetic strength, leptoquark masses up to 290 GeV are ruled out.

The ep collider HERA offers the unique possibility to search for resonant production of new particles which couple to lepton-parton pairs. Examples are leptoquarks (LQs), colour triplet bosons which appear naturally in various unifying theories beyond the Standard Model (SM). At HERA, leptoquarks could be singly produced by the fusion of the initial state lepton of energy 27.5 GeV with a quark from the incoming proton of energy up to 920 GeV, with masses up to the centre-of-mass energy $\sqrt{s_{ep}}$.

This analysis presents a search for LQs coupling to first generation fermions using e^+p data collected at $\sqrt{s_{ep}} = 300$ GeV, e^-p data collected at $\sqrt{s_{ep}} = 320$ GeV, and e^+p data collected at $\sqrt{s_{ep}} = 320$ GeV. These data sets correspond to integrated luminosities of 37 pb^{-1}, 15 pb^{-1} and 65 pb^{-1}, respectively. They represent the full statistics accumulated by the H1 experiment between 1994 and 2000. The e^+p and e^-p data sets are largely complementary when searching for leptoquark resonances, since the e^+p (e^-p) data provide most sensitivity to leptoquarks with fermion number $F = 0$ ($F = 2$), i.e. LQs coupling to e^+ (e^-) and a *valence* quark. The search reported here considers the decays $\mathrm{LQ} \rightarrow eq$ and $\mathrm{LQ} \rightarrow \nu q$ which lead to final states similar to those of deep-inelastic scattering (DIS) neutral current (NC) and charged current (CC) interactions at very high squared momentum transfer Q^2.

The phenomenology of LQs at HERA was discussed in detail in [1]. At HERA, LQs can be resonantly produced in the s-channel or exchanged in the u-channel between the incoming lepton and a quark coming from the proton. The amplitudes for both these processes interfere with those from DIS. We shall consider here the mass domain where the resonant s-channel contributions largely dominate the LQ signal cross-section.

In the s-channel, a LQ is produced at a mass $M = \sqrt{s_{ep}x}$ where x is the momentum fraction of the proton carried by the interacting quark. When the LQ decays into an electron and a quark, the mass is reconstructed from the measured kinematics of the scattered electron, and is henceforth labelled M_e. Similarly when the LQ decays into a neutrino and a quark, the mass is labelled M_h as it is reconstructed from the hadronic final state only [1].

The H1 detector components most relevant to this analysis are the liquid argon calorimeter, which measures the positions and energies of charged and neutral particles over the polar angular range[1] $4° < \theta < 154°$, and the inner tracking detectors which measure the angles and momenta of charged particles over the range $7° < \theta < 165°$. A full description of the detector can be found in [2].

This search relies essentially on inclusive NC and CC DIS selections. The selection of NC-like events follows that presented in [1]. It requires an identified electron with transverse momentum above 15 GeV and considers the kinematic domain defined by $Q^2 > 2500$ GeV^2 and $0.1 < y < 0.9$, where $y = Q^2/M^2$. The inelasticity variable y is related to the polar angle θ^* of the lepton in the centre-of-mass frame of the hard subprocess by $y = \frac{1}{2}(1 + \cos\theta^*)$. Since the angular distribution of the electron coming from the decay of a scalar resonance is markedly different from that of the scattered lepton in NC DIS [1], a mass dependent cut $y > y_{\mathrm{cut}}$ was applied previously [1, 3] to the e^+p 1994-1997 and e^-p 1998-1999 data in order to optimize the signal sensitivity. However, the optimization power is rather limited for a vector resonance as the angular distribution is only slightly different from that of the DIS background. This can be seen from the scattered event distribution in the mass$-y$ plane both for data (Fig. 1a,b) and

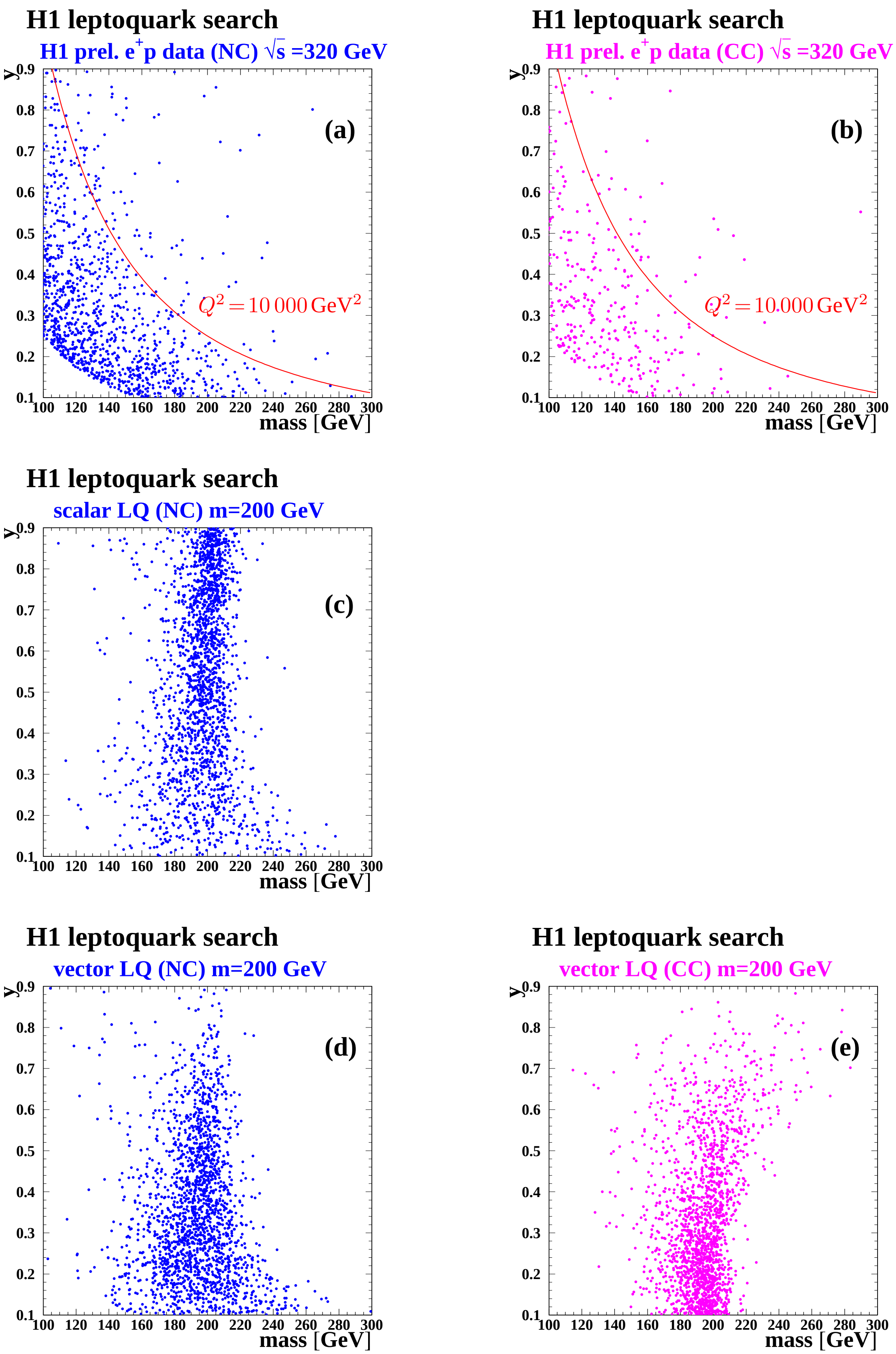

Figure 1: Data events selected in the NC (a) and CC (b) analyses and the corresponding Monte Carlo events at 200 GeV for (c) NC-like scalar, (d) NC-like vector LQs, and (e) CC-like vector LQ. In (a) and (b), the red lines are for shown value of Q^2 of $10\,000\,\mathrm{GeV}^2$.

for a 200 GeV NC-like scalar (vector) (Fig. 1c (1d)), and CC-like vector LQ (Fig. 1e). Indeed, from the ratio plot (Fig.2) of the LQ (signal) over the DIS background, one sees that applying a mass dependent y cut for a vector LQ can hardly improve the signal significance. For this reason, no y cut is applied in the analysis of the e^+p 1999-2000 data, instead bins with varying size adapted to the experimental resolution are defined in the mass-y plane to fully explore the signal sensitivity.

The mass spectrum measured in the $\sqrt{s_{ep}} = 320$ GeV data set is compared in Fig. 3a with the NC SM prediction, obtained using a Monte-Carlo calculation [4] and the MRST parametrization [5] for the parton densities. Similar mass spectrum of the NC DIS-like events measured in the 300 GeV e^+p and 320 GeV e^-p data sets and the comparison with the SM prediction can be found in [1, 3].

The selection of CC-like events follows closely that presented in [1, 6]. A missing transverse momentum exceeding 25 GeV and $Q^2 > 2500$ GeV^2 are required. The domain at high y where the resolution on the mass M_h degrades is removed by requiring $y < 0.9$. The observed and expected mass spectra are in good agreement as shown in Fig. 3b.

No evidence for LQ production is observed in the NC and CC data samples. Hence the data are used to set constraints on LQs which couple to first generation fermions. The e^-p data are used to set constraints on $F = 2$ LQs, and the NC data from both e^+p data sets are used to constrain LQs with $F = 0$.

For both the NC-like and CC-like channels, we use the numbers of observed and expected events and the signal efficiencies within the variable mass$-y$ bins for a given true LQ mass $M_{\rm LQ}$. Assuming Poisson distributions for the SM background expectations and for the signal, an upper limit on the number of events coming from LQ production is obtained using a modified frequentist approach [7]. This limit on the number of signal events is then translated into an upper bound on the LQ cross-section, which in turn leads to constraints on LQ models. The signal cross-section is obtained from the leading-order LQ amplitudes given in [8], corrected by multiplicative K-factors [9] to account for next-to-leading order QCD corrections. These corrections can enhance the LQ cross-section by $\mathcal{O}(10\%)$.

Both the statistical and the systematic errors are taken into account in the limit derivation. The main source of experimental systematic error considered is the uncertainty on the electromagnetic energy scale (between 0.7% and 3%) for the NC analysis, and the uncertainty on the hadronic energy scale (2%) for the CC analysis. Furthermore, an error of $\pm 7\%$ on the DIS expectations is attributed to the limited knowledge of proton structure. An additional systematic error arises from the theoretical uncertainty on the signal cross-section, originating mainly from the uncertainties on the parton densities. This uncertainty is 7% for $F = 2$ ($F = 0$) LQs coupling to e^-u (e^+u), and varies between 7% at low LQ masses up to 50% around 290 GeV for $F = 2$ ($F = 0$) LQs coupling to e^-d (e^+d). Moreover, choosing alternatively Q^2 or the square of the transverse momentum of the final state lepton instead of $M^2_{\rm LQ}$ as the hard scale at which the parton distributions are estimated yields an additional uncertainty of $\pm 7\%$ on the signal cross-section.

The phenomenological model proposed by Buchmüller, Rückl and Wyler (BRW) [8] describes 7 LQs with $F = 0$ and 7 LQs with $F = 2$. We use here the nomenclature of [11] to label

[1] The polar angle θ is defined with respect to the incident proton momentum vector (the positive z axis).

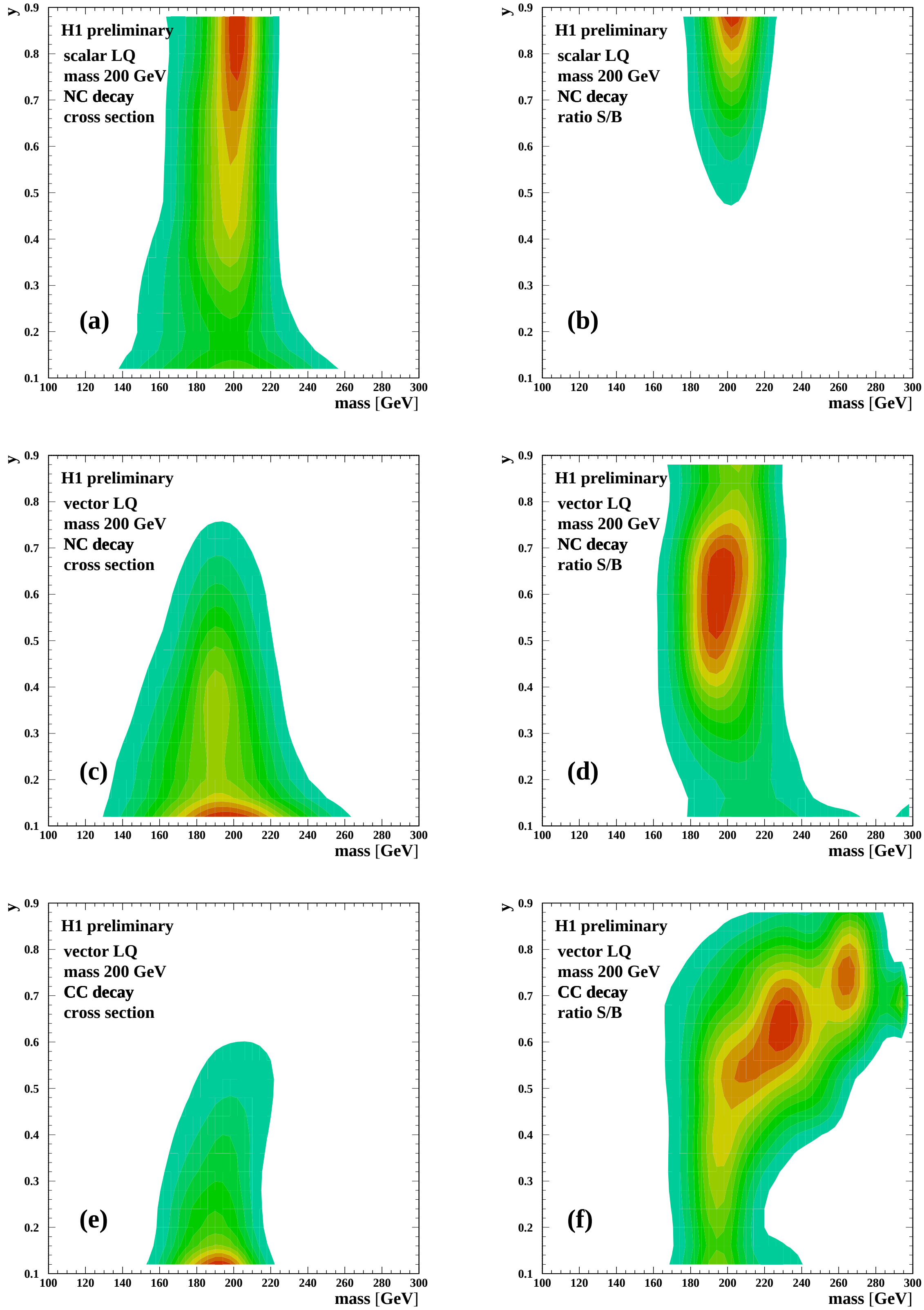

Figure 2: Leptoquarks (LQs) event distribution at 200 GeV for (a) NC-like scalar, (c) NC-like vector, and (e) CC-like vector LQs, and the corresponding signal over the Standard Model background ratios (b), (d), and (e).

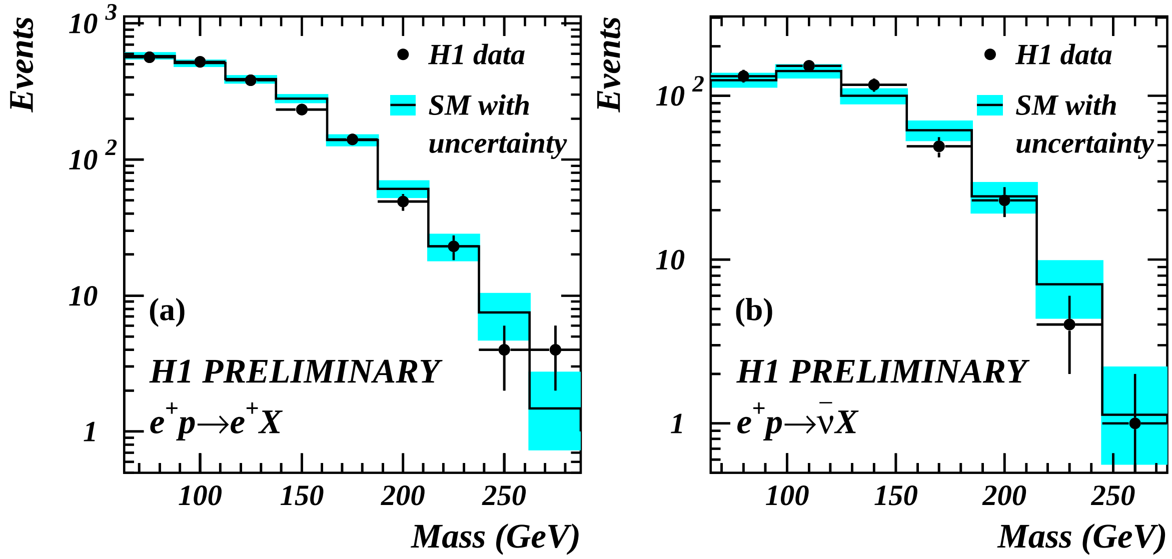

Figure 3: Mass spectra for the events from (a) neutral current (NC) and (b) charged current (CC) deep inelastic scattering (DIS) selections, together with the corresponding DIS expectations (histograms). The grey bands indicate the $\pm 1\sigma$ uncertainty due to the systematic errors on the NC and CC DIS expectations.

the various scalar $S_{I,L}$ ($\overset{(\sim)}{S}_{I,R}$) or vector $\overset{(\sim)}{V}_{I,L}$ ($V_{I,R}$) LQ types of weak isospin I, which couple to a left-handed (right-handed) electron. The tilde is used to distinguish LQs which differ only by their hypercharge. In the BRW model the branching ratios β_e (β_ν) for the LQ decays into eq (νq) are fixed and equal to 1 or 0.5 (0 or 0.5) depending on the LQ quantum numbers. Table 1 lists the 14 LQ types described by the BRW model.

For LQs with $F = 0$, the upper limits on the Yukawa coupling λ at the $e\,q$ LQ vertex obtained at 95% confidence level (CL) are shown as a function of the LQ mass in Figs. 4a and b, for scalar and vector LQs respectively. For masses above ~ 270 GeV, these bounds improve by a factor of about 5 the limits obtained in [1] from the analysis of e^+p data at $\sqrt{s_{ep}} = 300$ GeV. For mass values beyond the kinematic limit, the constraints from a contact interaction analysis [12] are also shown. Constraints corresponding to $F = 2$ LQs are shown in Figs. 4c and d. Constraints on LQs with masses above the HERA centre-of-mass energy were set in [1], where the interference between the LQ production and DIS processes was taken into account. These are shown in the rightmost part in Fig. 4c,d. For a Yukawa coupling of electromagnetic strength α_{em} ($\lambda = \sqrt{4\pi\alpha_{\text{em}}} = 0.3$) this analysis rules out LQ masses below 275 to 290 GeV, depending on the LQ type.

Fig. 5 summarizes the constraints on the $\tilde{S}_{1/2,L}$ and on the $S_{0,L}$ obtained by H1, by the L3 experiment at LEP [13], and by the Tevatron experiments [14]. For LQ masses above the HERA centre-of-mass energy, the H1 constraints obtained from a contact interaction approach [12] are also shown.

Beyond the BRW ansatz, generic LQ models can also be considered, where other LQ decay modes are allowed such that the branching ratios β_e and β_ν are free parameters. Mass dependent constraints on the LQ branching ratios can then be set for a given value of λ. For a scalar LQ possessing the quantum numbers of the $S_{1/2,L}$, which couples to e^+u, Fig. 6a shows the part

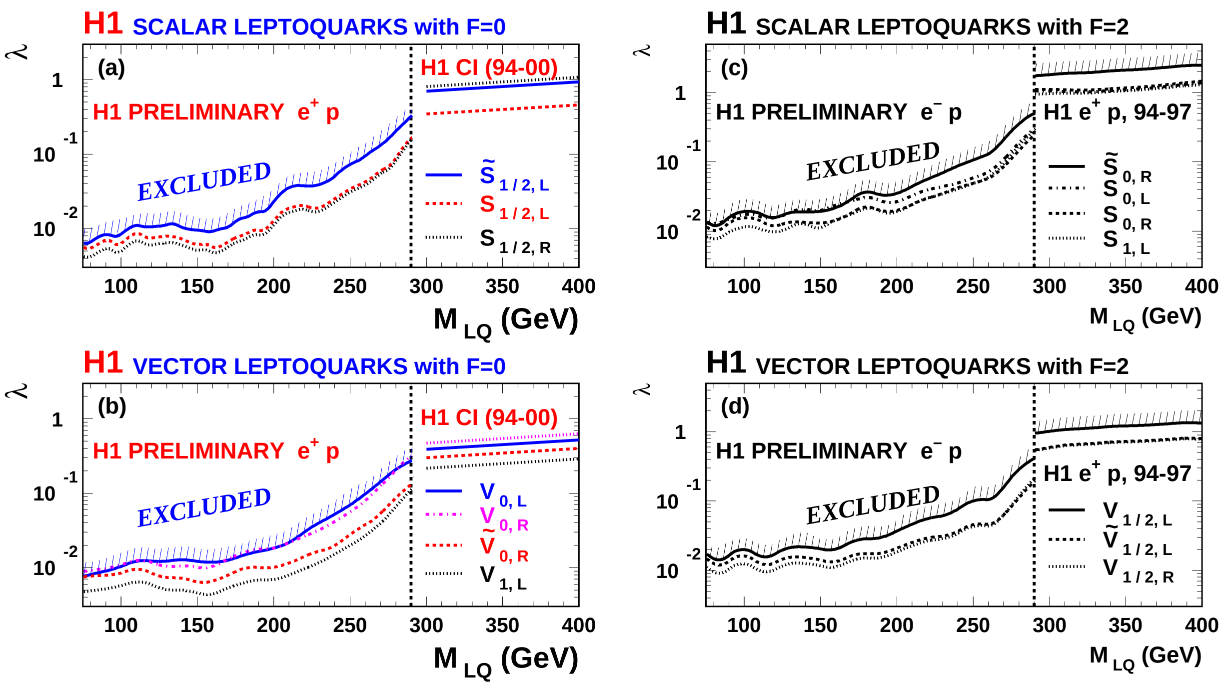

Figure 4: Exclusion limits for the 7 $F = 0$ leptoquarks (LQs) described by the Buchmüller, Rückl and Wyler (BRW) model. The limits are expressed at 95% CL on the Yukawa coupling λ as a function of the leptoquark mass for the (a) scalar LQs with $F = 0$, (b) vector LQs with $F = 0$, (c) scalar LQs with $F = 2$ and (d) vector LQs with $F = 2$. Domains above the curves are excluded. Constraints on LQs with masses above the HERA centre-of-mass energy, obtained from a contact interaction (CI) analysis and using the partial e^+p data sample at $\sqrt{s_{ep}} = 300$ GeV, are shown in the rightmost part of figures (a-b) and (c-d), respectively.

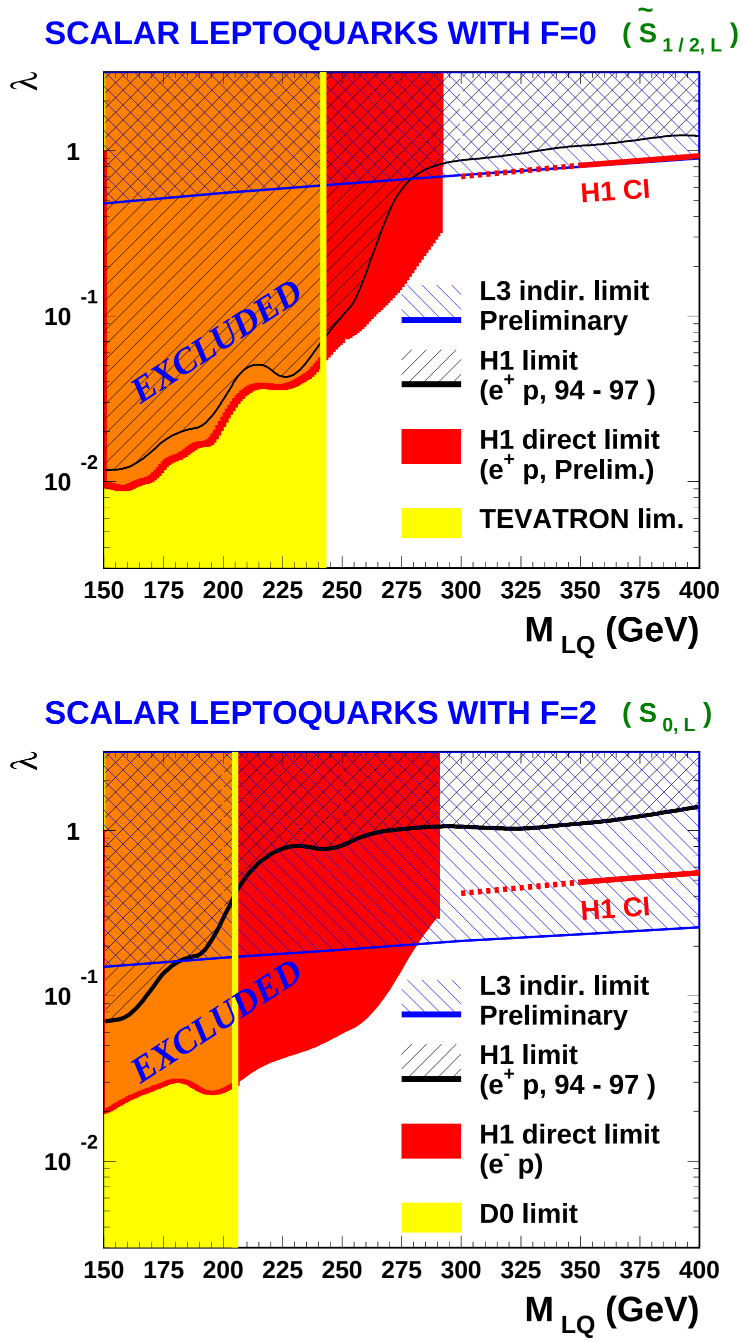

Figure 5: Exclusion limits at 95% CL on the Yukawa coupling λ as a function of the leptoquark (LQ) mass for (top) a scalar with $F = 0$ and (bottom) a scalar LQ with $F = 2$ described by the BRW model. Shaded and hatched domains are excluded.

$F=2$	Prod./Decay	β_e	$F=0$	Prod./Decay	β_e
			Scalar Leptoquarks		
${}^{1/3}S_0$	$e^-_L u_L \to e^- u$	$1/2$	${}^{5/3}S_{1/2}$	$e^+_R u_R \to e^+ u$	1
	$e^-_R u_R \to e^- u$	1		$e^+_L u_L \to e^+ u$	1
${}^{4/3}\tilde{S}_0$	$e^-_R d_R \to e^- d$	1	${}^{2/3}S_{1/2}$	$e^+_L d_L \to e^+ d$	1
${}^{4/3}S_1$	$e^-_L d_L \to e^- d$	1	${}^{2/3}\tilde{S}_{1/2}$	$e^+_R d_R \to e^+ d$	1
${}^{1/3}S_1$	$e^-_L u_L \to e^- u$	$1/2$			
			Vector Leptoquarks		
${}^{4/3}V_{1/2}$	$e^-_R d_L \to e^- d$	1	${}^{2/3}V_0$	$e^+_L d_R \to e^+ d$	1
	$e^-_L d_R \to e^- d$	1		$e^+_R d_L \to e^+ d$	$1/2$
${}^{1/3}V_{1/2}$	$e^-_R u_L \to e^- u$	1	${}^{5/3}\tilde{V}_0$	$e^+_L u_R \to e^+ u$	1
${}^{1/3}\tilde{V}_{1/2}$	$e^-_L u_R \to e^- u$	1	${}^{5/3}V_1$	$e^+_R u_L \to e^+ u$	1
			${}^{2/3}V_1$	$e^+_R d_L \to e^+ d$	$1/2$

Table 1: Leptoquark isospin families in the Buchmüller-Rückl-Wyler model. For each leptoquark, the superscript corresponds to its electric charge, while the subscript denotes its weak isospin. The leptoquarks are conventionally indexed with the chirality of the incoming *electron* which could mediate their production in e^-p collisions.

of the β_e-$M_{\rm LQ}$ plane which is ruled out by the NC analysis, for four values of the Yukawa coupling. For a vector LQ coupling to e^-d (possessing the quantum numbers of the $V_{0,L}$) and for $\lambda = 0.05$ and 0.3, the domain of the β_e-$M_{\rm LQ}$ (β_ν-$M_{\rm LQ}$) plane excluded by the NC (CC) analysis is shown in Fig. 6b. If the LQ decays into eq or νq only[2], the combination of both channels rules out the part of the plane on the left of the second and fourth full curves from the left, respectively for $\lambda = 0.05$ and 0.3. The resulting combined bound is largely independent of the individual values of β_e and β_ν. Combined bounds are also shown for $\lambda = 0.03$ and $\lambda = 0.1$. Fig. 6c shows exclusion areas in the same plane as for Fig. 6a, for a scalar LQ possessing the quantum numbers of the $\tilde{S}_{0,R}$ (which couples to e^-d). Fig. 6d shows similar exclusion limits as for Fig. 6(b), for a scalar LQ possessing the quantum numbers of the $S_{0,L}$ (which couples to e^-u). The domain excluded by the D0 experiment at the Tevatron [14] is also shown. For λ greater than ~ 0.03, the H1 limits extend considerably beyond the region excluded by the D0 experiment [14].

To summarize, a search for resonantly produced leptoquarks has been performed using all e^+p and e^-p data collected by H1 between 1994 and 2000. No signal has been observed and constraints on leptoquarks have been set, which extend beyond the domains excluded by other experiments. For a Yukawa coupling of electromagnetic strength, leptoquark masses up to 290 GeV can be ruled out.

[2]It should be noted that $\beta_e + \beta_\nu = 1$ does not imply $\beta_e = \beta_\nu$ even when invariance under $SU(2)_L$ transformations is required. For example, when LQs belonging to a given isospin multiplet are not mass eigenstates, their mixing usually leads to different branching ratios in both channels for the physical LQ states.

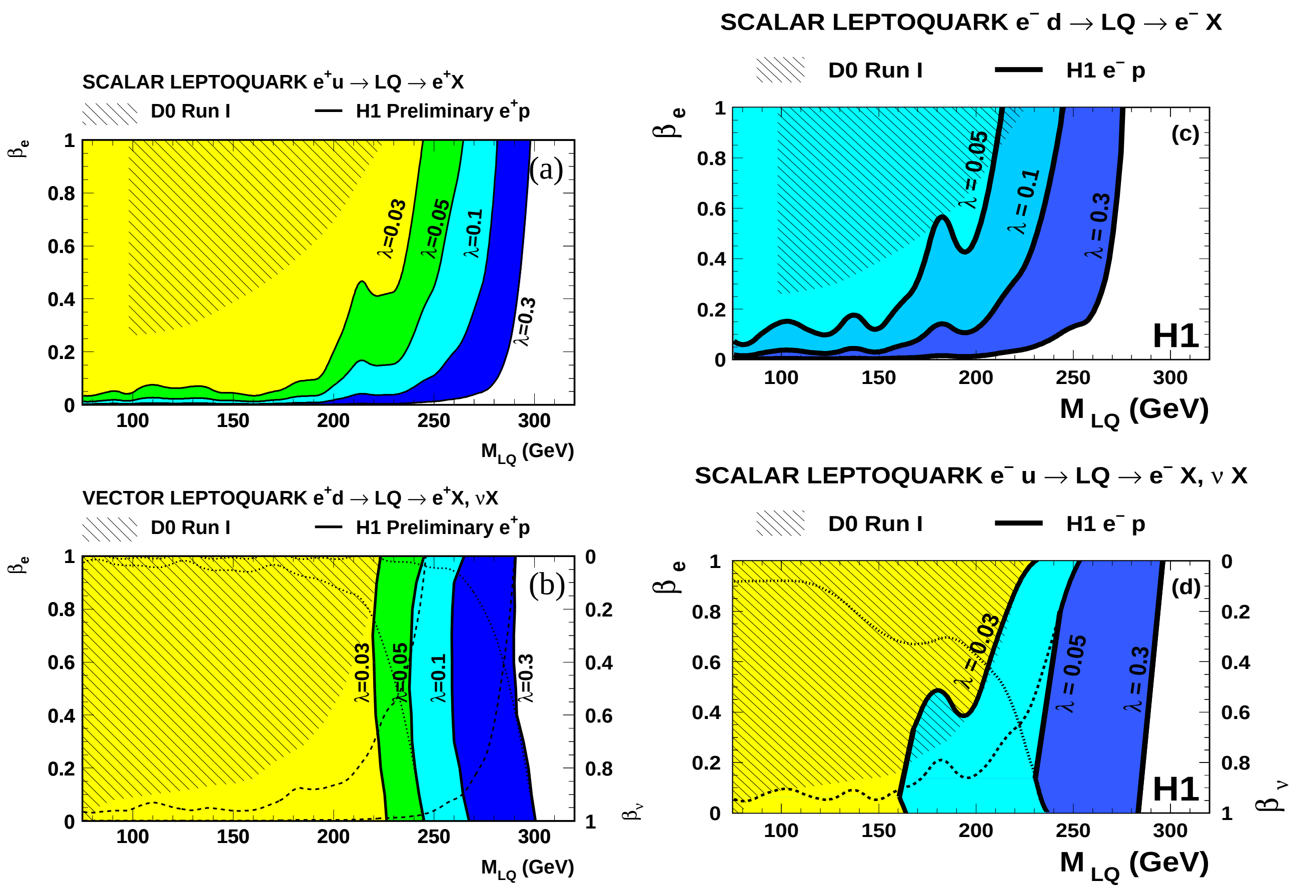

Figure 6: (a) Mass dependent exclusion limits at 95% CL on the branching ratio β_e of a scalar leptoquark (LQ) which couples to e^+u (with the quantum numbers of the $S_{1/2,L}$). (b) Domains ruled out by the combination of the NC and CC analyses, for a vector LQ which couples to e^+d (with the quantum numbers of the $V_{0,L}$) and decaying only into eq and νq for four values of the Yukawa coupling λ. (c) Same as for (a), here the scalar LQ couples to e^-d (with the quantum numbers of the $\tilde{S}_{0,R}$) [3]. (d) Same as for (b), here the scalar LQ couples to e^-u (with the quantum numbers of the $S_{0,L}$) [3]. The regions on the left of the full curves are excluded at 95% CL. For $\lambda = 0.05$ (also 0.3 in (b)), the part of the $\beta_e - M_{\rm LQ}$ ($\beta_\nu - M_{\rm LQ}$) plane on the left of the dashed (dotted) curve is excluded by the NC (CC) analysis. The branching ratios β_e and β_ν are shown on the left and right axes respectively. In (a-d), the hatched region represents the domain excluded by the D0 experiment. The D0 bounds do not depend on the value of the Yukawa coupling.

Acknowledgements

We are grateful to the HERA machine group whose outstanding efforts have made and continue to make this experiment possible. We thank the engineers and technicians for their work in constructing and now maintaining the H1 detector, our funding agencies for financial support, the DESY technical staff for continual assistance and the DESY directorate for the hospitality which they extend to the non DESY members of the collaboration.

References

[1] C. Adloff *et al.* [H1 Collaboration], Eur. Phys. J. C **11** (1999) 447 [Erratum-ibid. C **14** (1999) 553] [hep-ex/9907002].

[2] I. Abt *et al.* [H1 Collaboration], Nucl. Instrum. Meth. A **386** (1997) 310 and 348;
R. D. Appuhn *et al.* [H1 SPACAL Group Collaboration], Nucl. Instrum. Meth. A **386** (1997) 397.

[3] C. Adloff *et al.* [H1 Collaboration], Phys. Lett. B. **523** (2001) 234 [hep-ex/0107038].

[4] DJANGO 6.2; G.A. Schuler and H. Spiesberger, Proc. of the Workshop Physics at HERA, W. Buchmüller and G. Ingelman (Editors), (October 1991, DESY-Hamburg) Vol. 3 p. 1419.

[5] A. D. Martin, R. G. Roberts, W. J. Stirling and R. S. Thorne, Eur. Phys. J. C **4** (1998) 463 [hep-ph/9803445].

[6] C. Adloff *et al.* [H1 Collaboration], Eur. Phys. J. C **19** (2001) 269 [hep-ex/0012052].

[7] T. Junk, Nucl. Instrum. Meth. A **434** (1999) 435.

[8] W. Buchmüller, R. Rückl and D. Wyler, Phys. Lett. B **191** (1987) 442 [Erratum-ibid. B **448** (1999) 320].

[9] T. Plehn, H. Spiesberger, M. Spira and P. M. Zerwas, Z. Phys. C **74** (1997) 611 [hep-ph/9703433];
Z. Kunszt and W. J. Stirling, Z. Phys. C **75** (1997) 453 [hep-ph/9703427].

[10] T. Ahmed *et al.* [H1 Collaboration], Z. Phys. C **64** (1994) 545.

[11] A. Djouadi, T. Köhler, M. Spira and J. Tutas, Z. Phys. C **46** (1990) 679.

[12] H1 Collaboration, ICHEP'02 Contribution Paper 979.

[13] L3 Collaboration, Contribution paper no. 462 to ICHEP'02.

[14] B. Abbott *et al.* [D0 Collaboration], Phys. Rev. Lett. **79** (1997) 4321 [hep-ex/9707033];
B. Abbott *et al.* [D0 Collaboration], Phys. Rev. Lett. **80** (1998) 2051 [hep-ex/9710032].